

## Supporting information

### **Binding of Low-Molecular Weight Inhibitors Promotes Large Conformational Changes in the Dengue Virus NS2B-NS3 Protease – Fold-Analysis by Pseudocontact Shifts**

Laura de la Cruz, Thi Hoang Duong Nguyen, Kiyoshi Ozawa, James Shin, Bim Graham,  
Thomas Huber, Gottfried Otting

Reference 18:

Bodenreider, C.; Beer, D.; Keller, T. H.; Sonntag, S.; Wen, D.; Yap, L.; Yau, Y. H.; Geifman Shochat, S.; Huang, D.; Zhou, T.; Caflisch, A.; Su, X. C.; Ozawa, K.; Otting, G.; Vasudevan, S. G.; Lescar, J.; Lim, S. P. *Anal. Biochem.* **2009**, *395*, 195-204.

## Experimental Protocols

*Materials.* The dengue 2 NS2B-NS3pro construct used in the present work contained 255 residues, including a (Gly)<sub>4</sub>-Ser-(Gly)<sub>4</sub> linker between NS2B (47 residues) and NS3pro (185 residues).<sup>1</sup> In addition, it contained a His<sub>6</sub> tag at the C-terminus and the T7 gene 10 N-terminal peptide MASMTG at the N-terminus followed by a two-residue cloning artifact (LE), resulting in a 27 kDa protein. To suppress slow autocleavage detected by SDS-PAGE, most samples had the mutation Lys15Ala which caused no significant changes in the appearance of the NMR spectra. NS2B-C comprises the segment from Glu66\* to Leu95\* (to discriminate between NS2B and NS3 residues, residue numbers of NS2B are marked by an asterisk throughout this text). DENpro

samples were prepared either by cell-free protein synthesis from PCR-amplified DNA<sup>2</sup> or by high-cell density *in vivo* expression.<sup>3</sup>

Cell-free protein synthesis used the high-copy number plasmid pRSET-6d-DEN2 CF40GlyNS3pro as the template for PCR-amplification.<sup>1,4</sup> S30 cell extracts were prepared in-house from *E. coli* strains Rosetta::λDE3/pRARE and BL21 Star::λDE3,<sup>5</sup> including concentration with polyethylene glycol 8000. Heat treatment of the concentrated extracts at 42 °C<sup>5,6</sup> was applied in the early phase of the project but was later found to be non-essential for achieving high protein yields. <sup>15</sup>N-labeled amino acids were purchased from Cambridge Isotope Laboratories and ISOTECH. Synthetic oligonucleotides were purchased from IDT-DNA Technologies and Geneworks. PCRs were performed using *Vent* DNA polymerase (New England Biolabs). PCR products were purified using the QiaQuick PCR purification kit (Qiagen).

*In vivo* expression experiments used the same gene constructs as cell-free expression but inserted into the pETMCSI T7 expression vector<sup>7</sup> and transformed into the *E. coli* strain Rosetta::λDE3/pRARE.

The C1- and C2-compounds for tagging with lanthanides were synthesized as described.<sup>8</sup>

*Cell-Free Protein Synthesis.* DNA templates encoding the double mutant Lys117Arg/Thr122Arg and the sixteen possible single Ile-to-Val mutants were prepared closely following a published protocol,<sup>2</sup> except that the heating period in the re-annealing step was extended to 10 minutes. Samples of DENpro were synthesized in a cell-free *E. coli* coupled transcription-translation system using a previously described

protocol.<sup>5,9</sup> <sup>15</sup>N-labeled isoleucine was used in the cell-free reaction mixture. Wild-type DENpro was synthesized using the pRSET-DEN2 CF40GlyNS3pro plasmid at a concentration of 16 µg/ml of reaction mixture. Mutant DENpro was synthesized using re-annealed DNA at a concentration of 20 µg/ml of reaction mixture. Each synthesis was performed in three identical parallel reactions, each using a reaction volume of 0.5 ml in 5 ml of outer buffer and proceeding for 14-15 h at 30 °C.

The S30 extract used for the expression of selectively <sup>15</sup>N-serine labeled samples was reduced with sodium borohydride to suppress cross-labeling by transaminases as described previously.<sup>10</sup> 100-150 µM NMR samples were obtained from three 2.5 ml reactions in 25 ml of outer buffer at 30 °C in overnight reactions (14-15 h).

*Protein Purification.* Following synthesis, the protein samples were purified using IMAC Ni-NTA spin columns. The columns were equilibrated with binding buffer (50 mM Na<sub>3</sub>PO<sub>4</sub>, 300 mM NaCl, 10 mM imidazole at pH 7.4), loaded with the sample, washed five times with wash buffer (50 mM Na<sub>3</sub>PO<sub>4</sub>, 300 mM NaCl, 30 mM imidazole, pH 7.4), and eluted with elution buffer (50 mM Na<sub>3</sub>PO<sub>4</sub>, 300 mM NaCl, 300 mM imidazole, pH 7.4). The purified protein was washed with NMR buffer (20 mM Tris HCl, 30 mM NaCl, pH 6.9) or, in the case of the <sup>15</sup>N-serine labeled samples, MES buffer (20 mM MES, 30 mM NaCl, pH 6.5) and the samples were concentrated to 500 µl using a Centricon-4 ultrafilter MWCO-10 kDa concentrator (Amicon).

*Tagging Reaction.* C1- and C2-tags loaded with Tb<sup>3+</sup>, Tm<sup>3+</sup> or Y<sup>3+</sup> (Figure 2) were attached to the single cysteine mutants of DENpro by adding the protein to a three-fold excess of the respective metal complexes of C1 or C2 in NMR buffer and incubating at

room temperature overnight. After incubation, the samples were centrifuged at 4 °C for 30 min. Excess low-molecular weight reactants and products were removed by concentration and dilution with NMR buffer.

*NMR Spectroscopy.* All NMR spectra were recorded at 25 °C on Bruker 600 and 800 MHz NMR spectrometers equipped with cryoprobes. NMR spectra were recorded either in NMR buffer or in 20 mM MES buffer. Most experiments used *p*-nitrophenyl-*p*-guanidino benzoate (referred to as compound **1** in Figure 2) as an inhibitor.<sup>11</sup> **1** was added in five-fold molar excess to the protein using a 100 mM stock solution in DMSO- $d_6$ .

*Resonance Assignment of DENpro with and without Inhibitor 1.* 3D NMR spectra of a uniformly  $^2\text{H}/^{15}\text{N}/^{13}\text{C}$ -labeled sample were recorded using TROSY versions of HN(CO)CA, HNCACB and HNCO. In addition, HNCA and NOESY- $^{15}\text{N}$ -HSQC (80 ms mixing time) spectra were recorded of  $^{15}\text{N}/^{13}\text{C}$ -labeled and  $^{15}\text{N}$ -labeled samples, respectively.

The residue type of the  $^{15}\text{N}$ -HSQC cross-peaks was identified by five combinatorially  $^{15}\text{N}$ -labeled samples produced by cell-free protein synthesis following an established protocol.<sup>10,12,13</sup> In addition, 2D HN(CO) spectra were recorded of five samples prepared with uniform  $^{15}\text{N}$ -labeling and simultaneous combinatorial  $^{13}\text{C}$ -labeling to identify the preceding residue type for each of the cross-peaks in the  $^{15}\text{N}$ -HSQC spectrum.

*Homology Model of the Closed Conformation of DENpro.* The NS2B-NS3 proteases from dengue and West Nile virus share over 50% sequence identity and similar structures have been reported for both proteins in the absence of inhibitors.<sup>1,14</sup> Using the

software Modeller,<sup>15,16</sup> we built a model of DENpro in the inhibitor-bound state using as templates the crystal structures of WNVpro in complex with different inhibitors (PDB codes 2FP7, 3E90, and 2IJO<sup>1,14,17</sup>) and the crystal structure of DENpro in the absence of inhibitor (PDB code 2FOM<sup>1</sup>). The sequence alignment was generated using ClustalX,<sup>18</sup> excluding residues for which no electron density had been observed in the crystal structures. The peptide inhibitor Bz-Nle-K-R-R-H<sup>1</sup> was included in the target structure. 1000 models were built and ranked by the internal Discrete Optimized Protein Energy (DOPE) function.<sup>19</sup> The ten best models of DENpro showed a similar DOPE profile, indicating convergence. The best model had a C<sup>α</sup> RMSD of 0.5 Å (162 residues superimposed) and 0.7 Å (140 residues superimposed) to 2FP7 and 2FOM, respectively. It is very similar to a previously published model (C<sup>α</sup> RMSD of 0.8 Å following superimposition of 193 residues).<sup>20</sup> The coordinates are available from <http://rsc.anu.edu.au/~go/coordinates/>.

*Fitting of  $\Delta\chi$  Tensors.* PCSs were measured as the difference in <sup>1</sup>H chemical shifts of the backbone amides observed in <sup>15</sup>N-HSQC spectra of paramagnetic versus diamagnetic samples. The PCS  $\Delta\delta^{\text{PCS}}$  of a nuclear spin depends on its polar coordinates  $r$ ,  $\theta$  and  $\varphi$  with respect to the principal axes of the magnetic susceptibility anisotropy tensor ( $\Delta\chi$  tensor):<sup>21</sup>

$$\Delta\delta^{\text{PCS}} = \frac{1}{12\pi r^3} \left[ \Delta\chi_{\text{ax}} (3\cos^2\theta - 1) + \frac{3}{2} \Delta\chi_{\text{rh}} \sin^2\theta \cos 2\varphi \right] \quad (1)$$

where  $\Delta\chi_{\text{ax}}$  and  $\Delta\chi_{\text{rh}}$  denote, respectively, the axial and rhombic components of the  $\Delta\chi$  tensor. The principal axes system of the  $\Delta\chi$  tensor of each paramagnetic sample was determined by fitting to the model of DENpro described above.

Fits were performed as described earlier.<sup>8,22</sup> Briefly, the structure of DENpro with bound C1- or C2-tag was modeled and several million different conformations were generated by randomly changing the dihedral angles of the cysteine side chain, the disulfide bond and the ethylene tether of the tag, using dihedral angles of 60°, -60°, and 180° for the C-C bonds and dihedral angles of -90° or 90° for the S-S bond, with an uncertainty range of  $\pm 10^\circ$ . Conformations producing steric clashes with the protein were excluded. The remaining conformers were used to fit  $\Delta\chi$  tensors to the experimental PCSs. The final  $\Delta\chi$  tensor was taken to be the one obtained with the conformation producing the best least square fit to the experimentally observed PCS data. The program Numbat<sup>23</sup> was used to back-calculate PCSs from fitted  $\Delta\chi$  tensors and to generate the isosurfaces shown in Figure 9.

*Mass Spectrometry.* Mass spectra were obtained with a Bruker 4.7 T ESI-FT-ICR mass spectrometer with the following parameters for ionization and ion transfer: capillary -3888 V, end plate -3788 V, capillary exit 150 V, skimmer I 13.3 V, skimmer II 8.36 V, r.f. amplitude 580.0 Vpp, dry gas temperature 120 °C, trap 11.06 V, extract -6.31 V, ICR trap voltage 0.85 V, data size 512K, mass range  $m/z$  500–2000. Spectra were acquired in broadband mode accumulating 50-500 scans and the  $m/z$  scale was calibrated using PEG1500. Samples were 20  $\mu\text{M}$  in 1:1 methanol:water with 0.5% (v/v) formic acid and infused at a flow rate of 100  $\mu\text{l/h}$ .

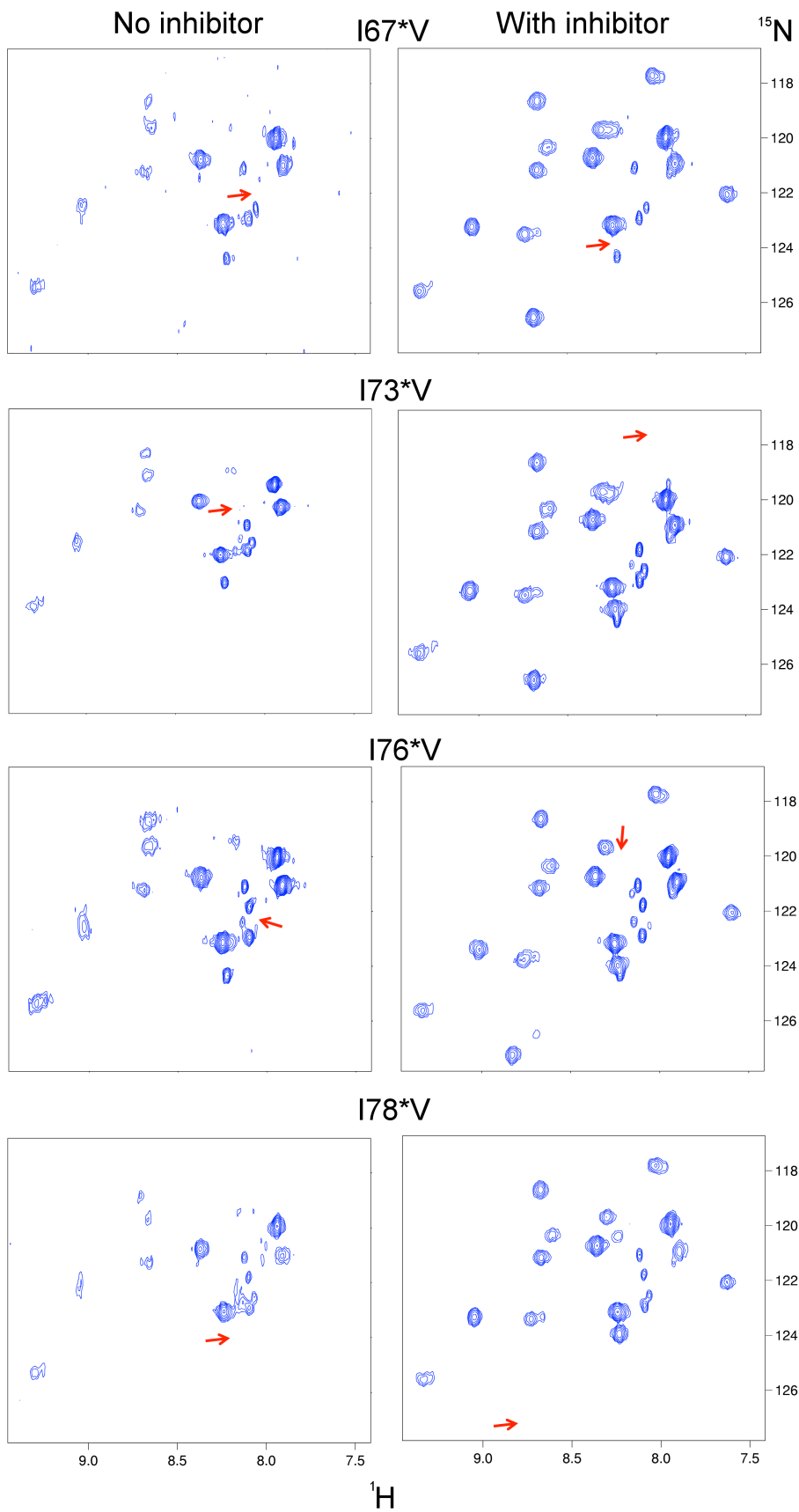


Figure S1 continued

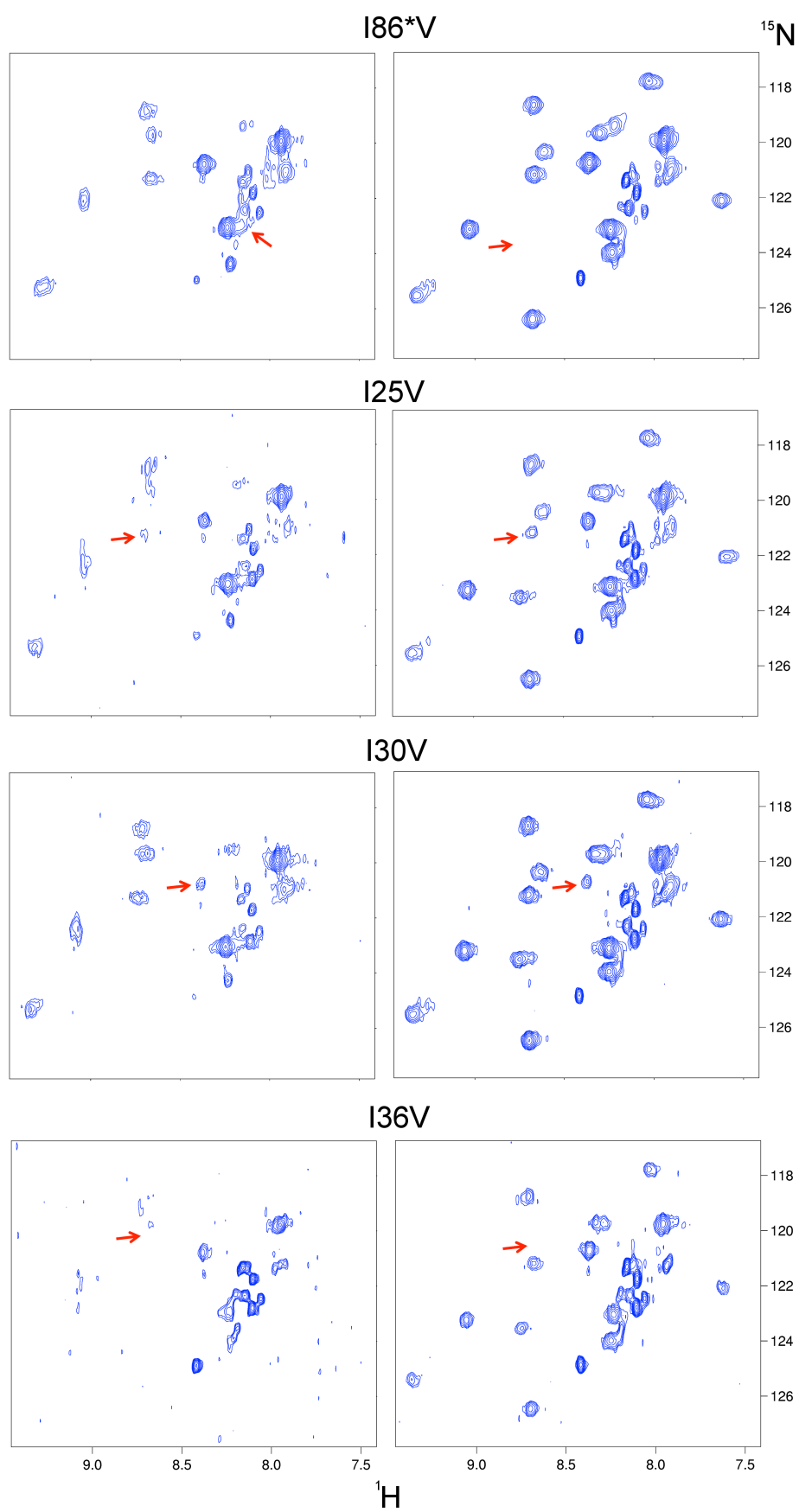


Figure S1 continued

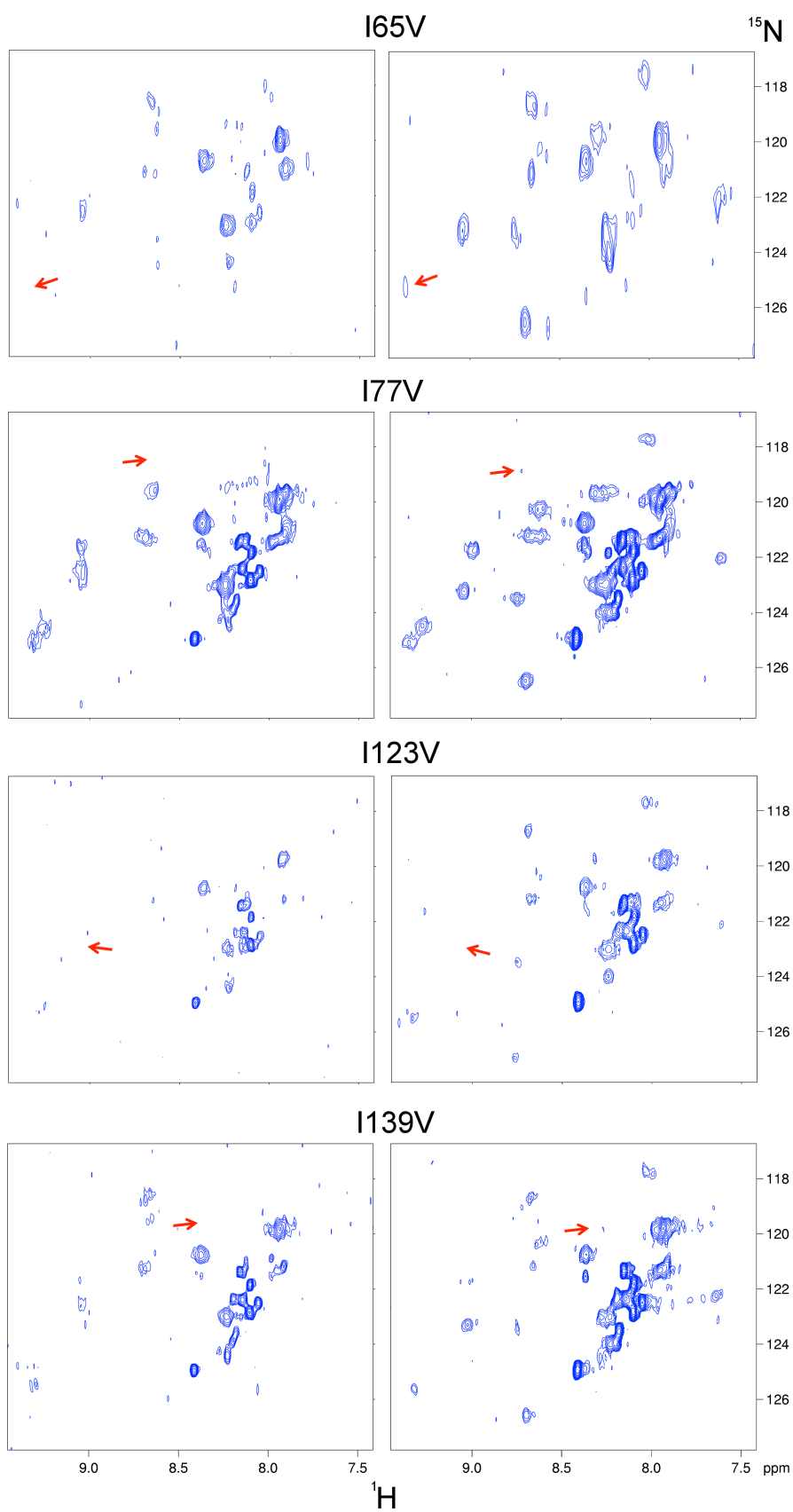
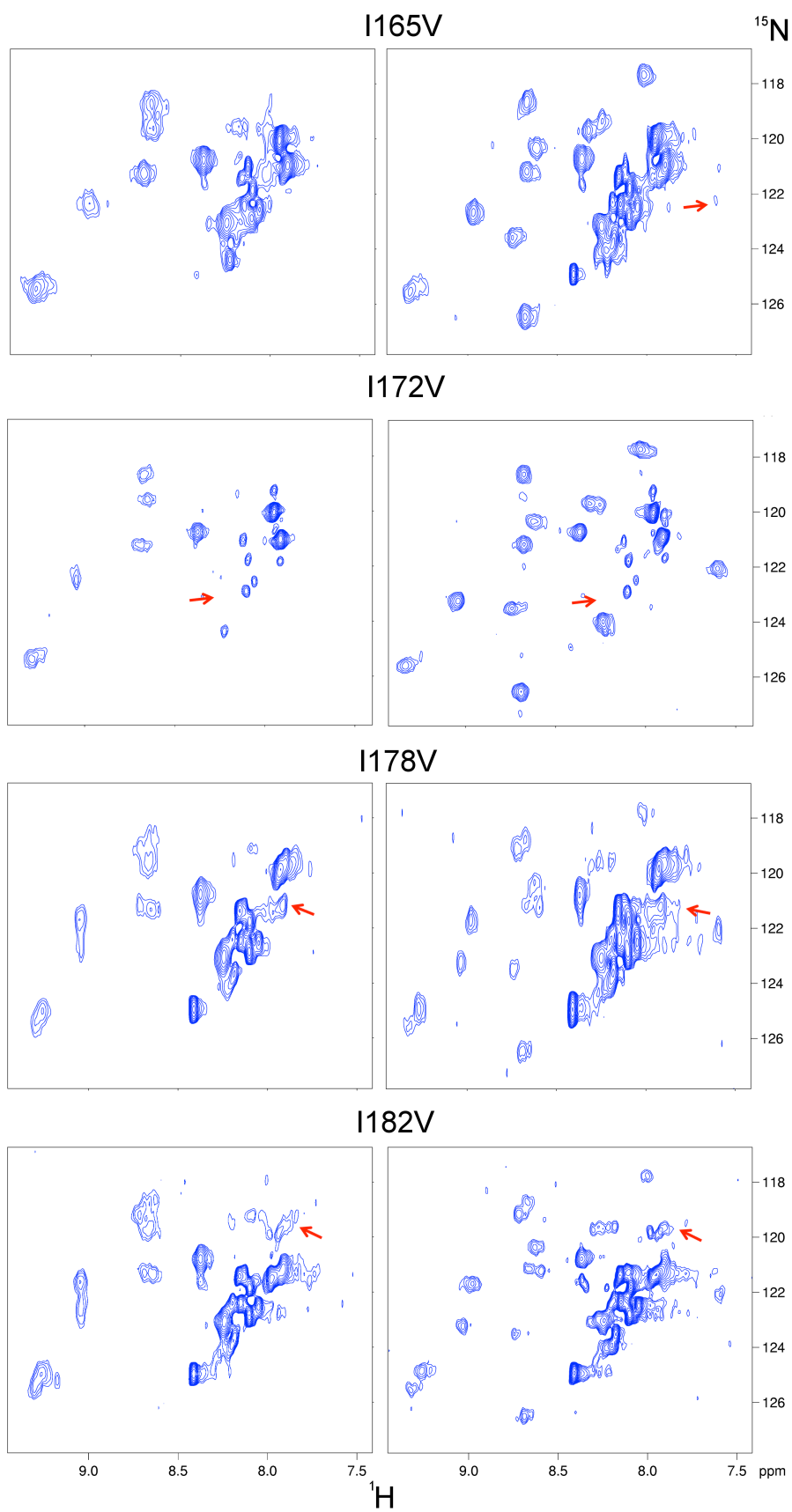


Figure S1 continued



**Figure S1.** Resonance assignment of isoleucine amides by mutation. The figure shows

<sup>15</sup>N-HSQC spectra of each of the 16 Ile to Val mutants of DENpro at pH 6.9 and 25 °C without (left panel) and with (right panel) a five-fold excess of the inhibitor 4-guanidino-benzoic acid-4-nitrophenyl ester (inhibitor **1**). Red arrows identify the positions of cross-peaks that were weaker due to mutation, identifying the resonance assignments in the spectrum of the wild-type protein. The assignments made in the absence of inhibitor agree with the previously published assignments.<sup>2</sup> In addition, they assign the cross-peak at 9.05 ppm to Ile123. The cross-peak of Ile165 could only be identified in the presence of **1**.

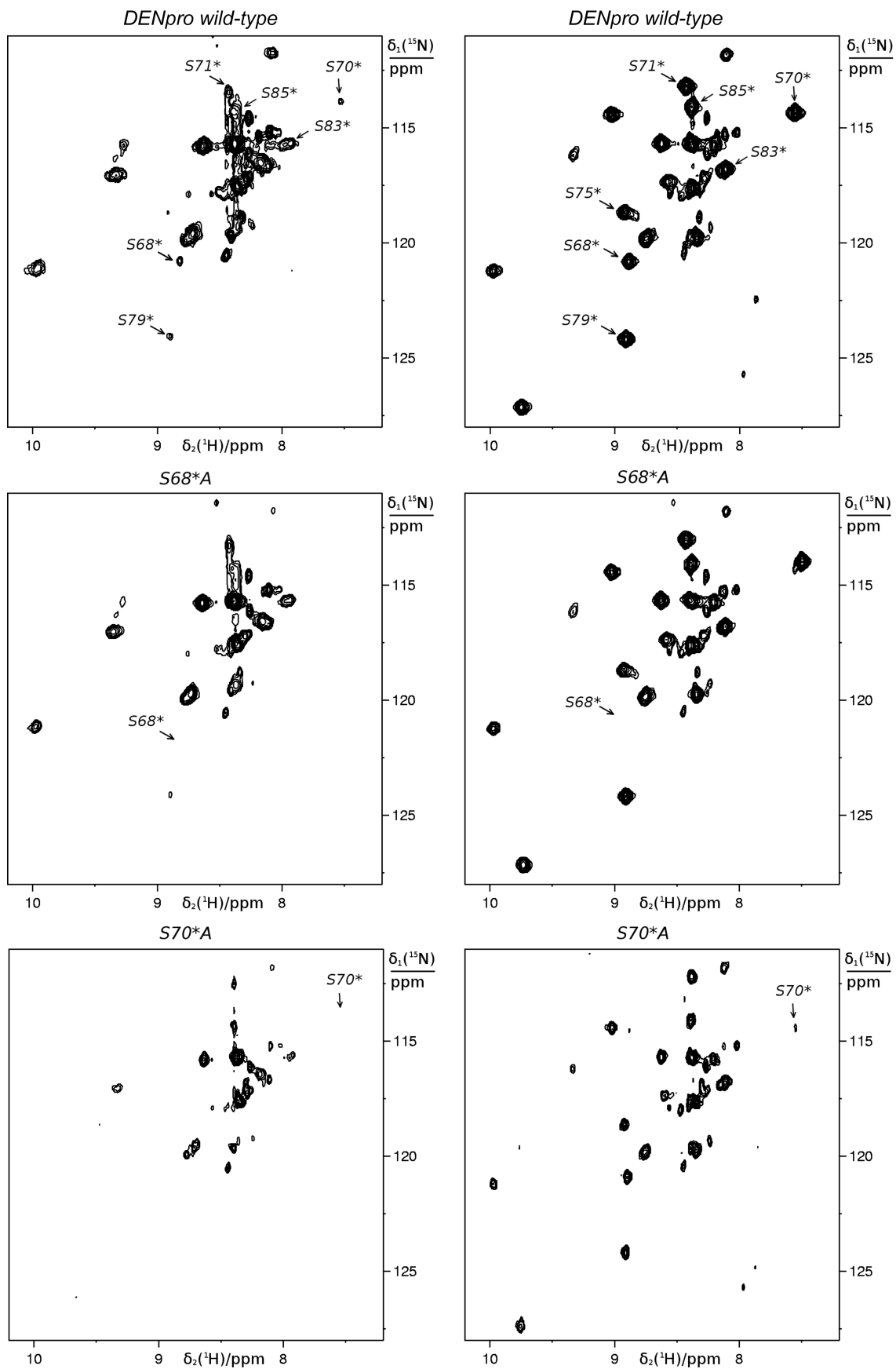


Figure S2 continued

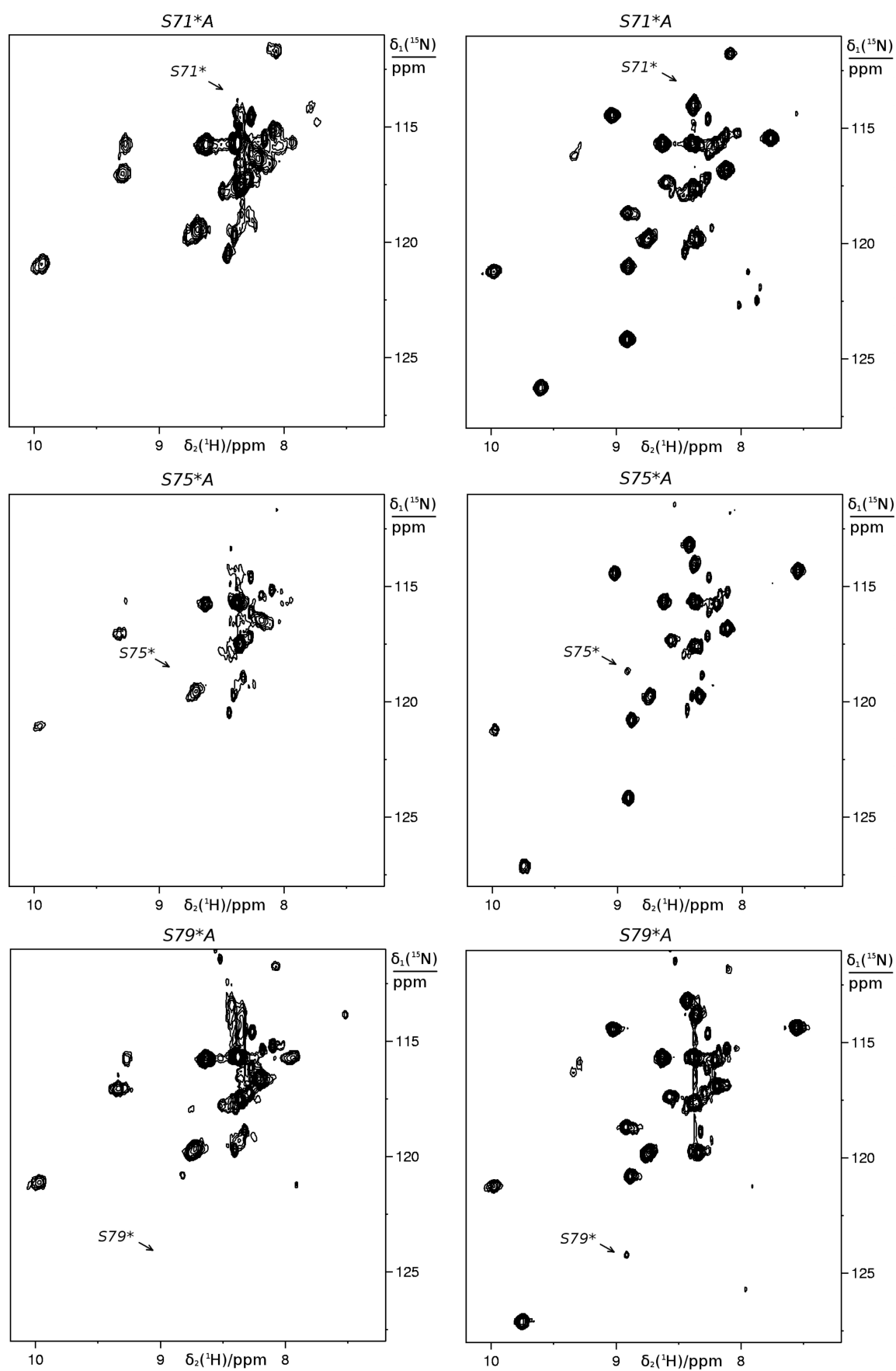
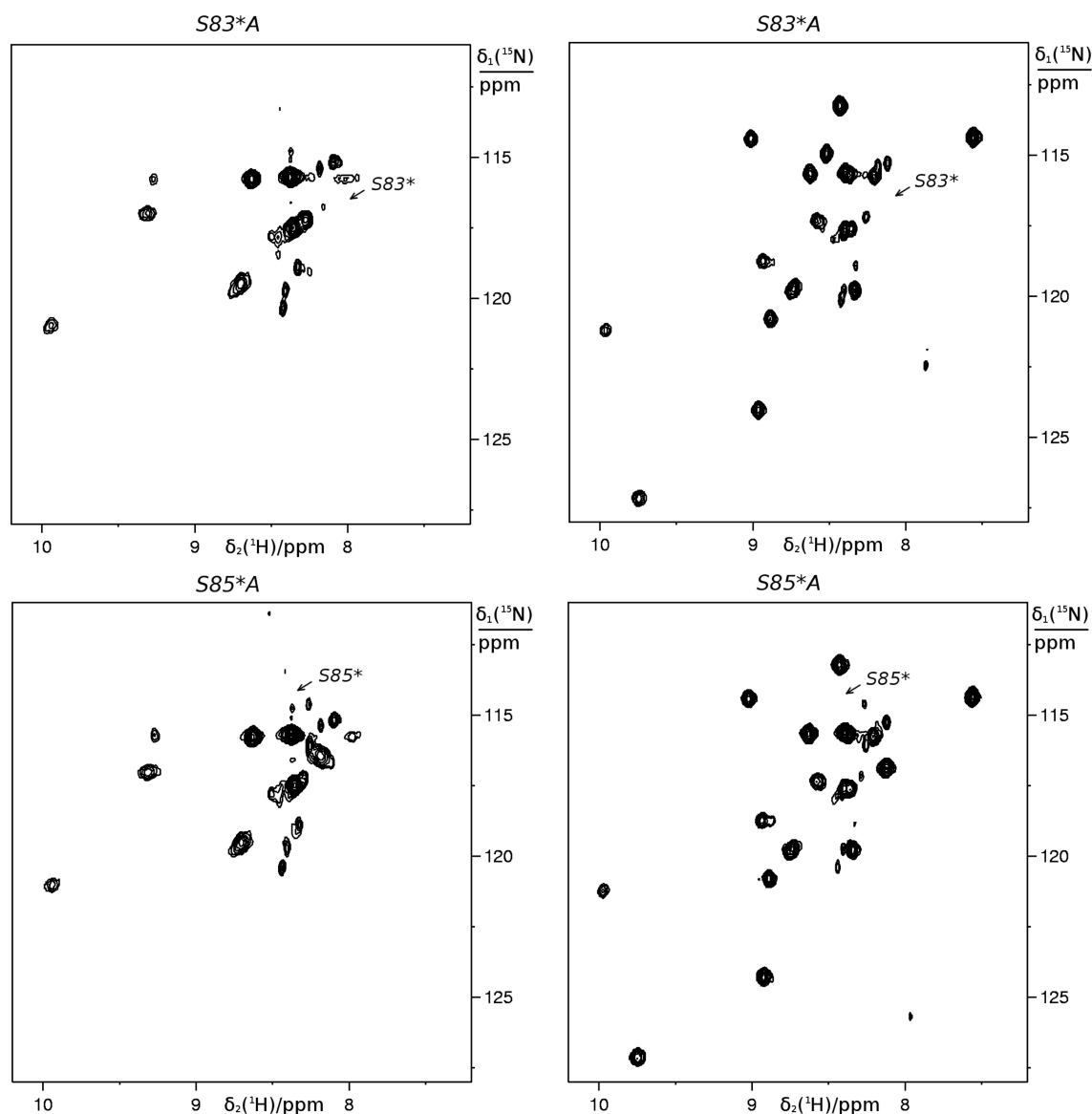
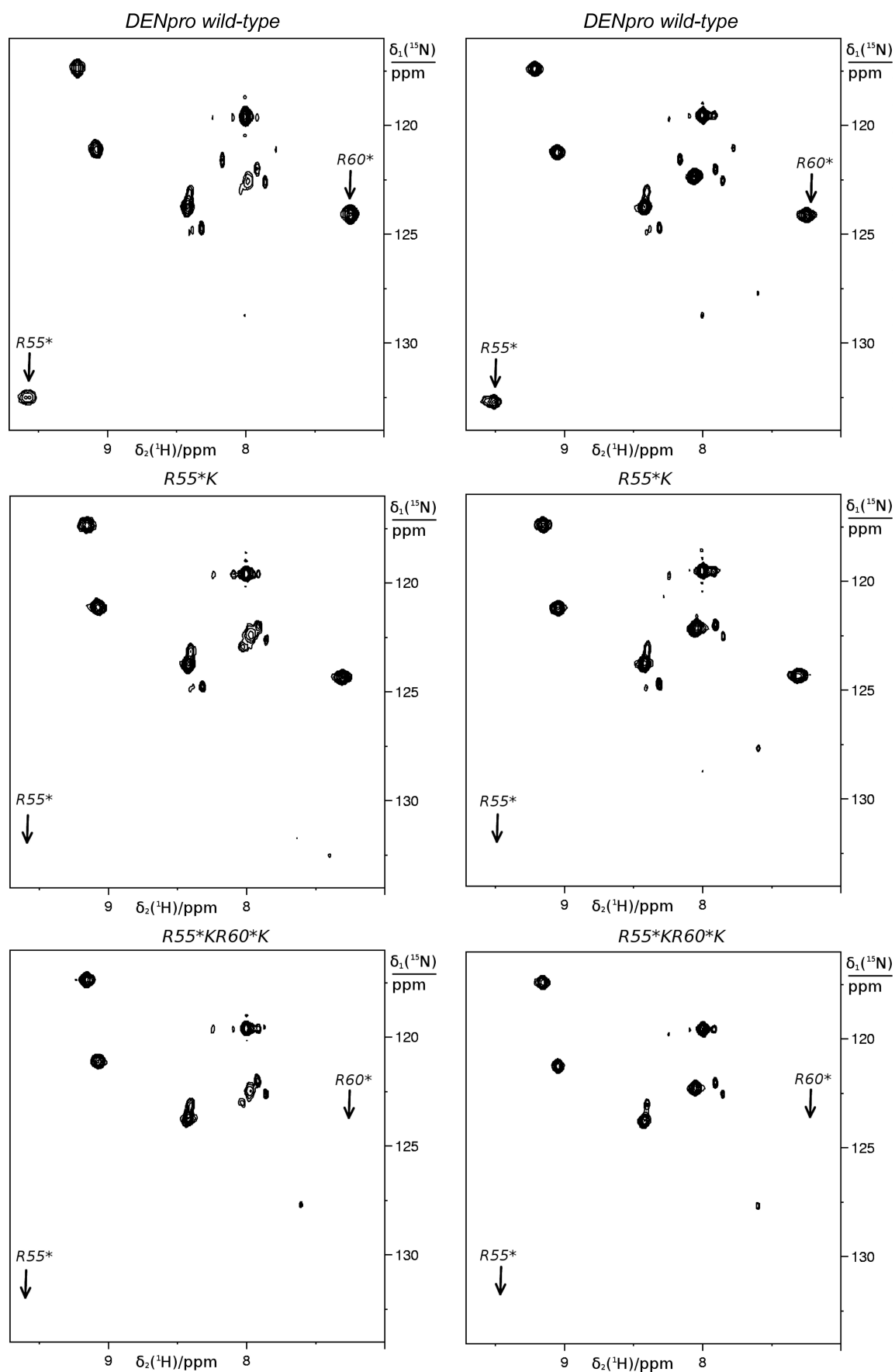


Figure S2 continued



**Figure S2.** Resonance assignment of serine amides of NS2B by mutation. The figure shows  $^{15}\text{N}$ -HSQC spectra of seven Ser to Ala mutants of DENpro at pH 6.5 and 25 °C without (left panel) and with (right panel) a five-fold excess of the inhibitor **1**. Arrows in the spectra with inhibitor identify the positions of cross-peaks that were weaker due to mutation, identifying the resonance assignments in the spectrum of the wild-type protein shown in the top panel. The arrows were reproduced in the spectra of the left panel, showing that cross-peaks at the corresponding positions were much weaker or absent in the protein without bound inhibitor.



**Figure S3.** Resonance assignment of arginine amides of NS2B by mutation. The figure

shows  $^{15}\text{N}$ -HSQC spectra of two Arg to Lys mutants of DENpro at pH 6.5 and 25 °C without (left panel) and with (right panel) a five-fold excess of the inhibitor **1**. Arrows identify the positions of cross-peaks which were absent due to mutation, identifying the resonance assignments in the spectrum of the wild-type protein shown in the top panel.

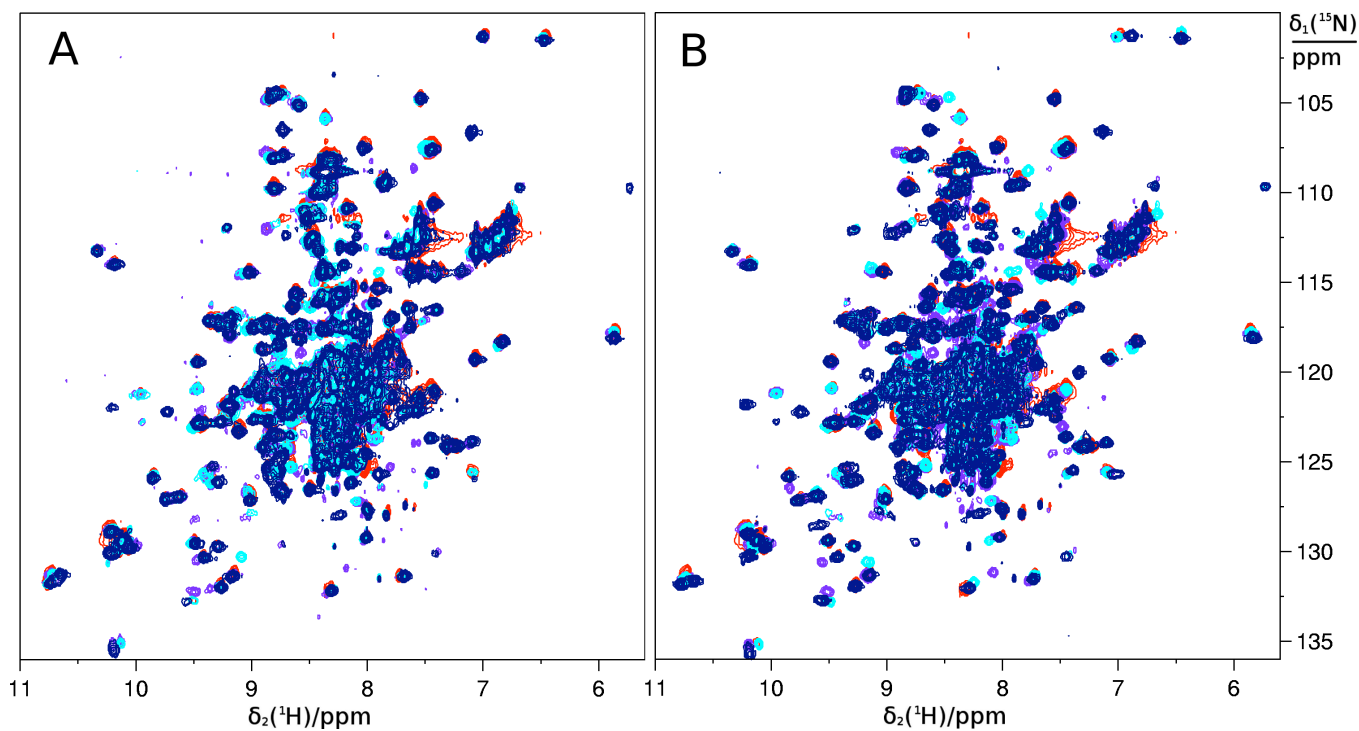


**Figure S4.** Introduction of tags into DENpro at sites A-C does not change the structure of the protein. The figure shows the  $^{15}\text{N}$ -HSQC spectra of the mutants A (purple), B (cyan), C (blue) superimposed onto the  $^{15}\text{N}$ -HSQC spectrum of the wild-type protein DENpro (red). (A) Mutants labeled with diamagnetic C1- $\text{Y}^{3+}$ -tags. (B) Same as (A), except for C2- $\text{Y}^{3+}$ -tags. All spectra were recorded in the presence of a five-fold excess of **1**. Chemical shift changes between the spectra are restricted to few cross-peaks, confirming that the tags perturbed the chemical environment only locally, leaving the fold of the protein intact.

**Table S1.** PCSs in ppm of backbone amide protons of  $^{15}\text{N}$ -labeled DENpro Ala57\*Cys (mutant A) tagged with C1 or C2 loaded with  $\text{Tb}^{3+}$  or  $\text{Tm}^{3+}$  <sup>a</sup>

Residue	C1		C2	
	$\text{Tb}^{3+}$	$\text{Tm}^{3+}$	$\text{Tb}^{3+}$	$\text{Tm}^{3+}$
70* SER	0.192	-0.253		
71* SER	0.133	-0.098	0.363	-0.287
75* SER	0.053	-0.051	0.121	-0.087
78* ILE	0.056	-0.035	0.062	-0.027
79* SER	0.046	-0.034	0.018	-0.007
82* GLY	0.048	-0.017	-0.005	0.004
83* SER	0.047	-0.028	-0.006	0.007
85* SER	0.078	-0.033		
26 LYS	-0.411	0.324		
28 LYS	-0.204	0.169	-0.581	0.461
29 GLY	-0.148	0.115		
34 SER	-0.203	0.195		
39 GLY	-0.254	0.279	-0.641	0.730
41 TYR				0.399
47 HIS	-0.117	0.156	-0.233	0.230
50 TRP	0.010	-0.018	-0.101	0.086
51 HIS		0.018	-0.130	0.113
52 VAL	-0.006	0.039	-0.222	0.188
53 THR	-0.065	0.057	-0.271	0.227
55 GLY	-0.053	0.064	-0.217	0.177
56 ALA			-0.262	0.212
62 GLY	-0.332	0.239	-0.711	0.391
65 ILE	-0.202	0.175	-0.320	0.277
70 ALA			-0.038	0.047
71 ASP	0.036	0.017		
74 LYS	0.077	0.005	0.019	-0.019
76 LEU	0.062	-0.008	-0.020	0.027
77 ILE	0.026	0.017		
79 TYR	-0.115	0.098		
82 GLY	-0.034	0.036	-0.005	0.020
85 LEU	0.090	-0.045	0.142	-0.083
89 TRP	0.286	-0.229		
112 LYS	0.305	-0.234	0.694	-0.535
114 GLY	0.233	-0.170	0.399	-0.297
116 PHE	0.149	-0.111	0.210	-0.161
117 LYS	0.098	-0.064		
121 GLY	0.078	-0.059	0.097	-0.079
122 THR	0.108	-0.075	0.142	-0.109
123 ILE	0.137	-0.096	0.178	-0.133
127 SER	0.293	-0.208		

128	LEU	0.293	-0.221	0.415	-0.305
130	PHE	0.240	-0.177		
131	SER	0.251	-0.147		
133	GLY			-0.526	0.417
148	GLY	0.423	-0.346	0.563	-0.411
159	GLY		-0.096		
160	ALA			0.135	-0.097
166	ALA			0.254	-0.165

<sup>a</sup> PCSs were measured as the chemical shift of the paramagnetic species minus the chemical shift of the same mutant tagged with the corresponding diamagnetic tag loaded with Y<sup>3+</sup>. Sequence numbers of NS2B residues are labeled with a star. When  $\Delta\chi$  tensors were fitted to NS3pro, PCSs from NS2B residues with sequence numbers below 60\* were included in the NS3pro data set because those residues are unaffected by the conformational change of NS2B-C. The data were measured in <sup>15</sup>N-HSQC spectra of 0.1-0.2 mM protein solutions in NMR buffer at 25 °C.

**Table S2.** PCSs in ppm of backbone amide protons of <sup>15</sup>N-labeled DENpro Ser34Cys (mutant B) tagged with C1 or C2 loaded with Tb<sup>3+</sup> or Tm<sup>3+</sup> <sup>a</sup>

Residue	C1		C2	
	Tb <sup>3+</sup>	Tm <sup>3+</sup>	Tb <sup>3+</sup>	Tm <sup>3+</sup>
55* ARG	-0.476	0.358	-0.637	0.587
56* ALA	-0.238	0.198	-0.286	
62* GLU	0.022	-0.016	0.052	-0.038
63* GLU			0.027	-0.027
64* GLN			0.046	-0.040
65* ALA	0.065	-0.037	0.073	-0.056
67* ILE	0.108		0.110	
68* SER			0.103	-0.077
70* SER	0.146	-0.093	0.176	-0.155
71* SER	0.105	-0.066	0.126	-0.111
73* ILE	0.116		0.123	
75* SER	0.113	-0.064	0.114	-0.132
78* ILE	0.147		0.248	
79* SER	0.212	-0.138	0.370	-0.321
82* GLY	0.252	-0.162	0.480	-0.412
85* SER	0.212	-0.126	0.311	-0.251

86*	ILE	0.199		0.202	
21	GLY	-0.239	0.172	-0.223	0.200
22	ALA	-0.203	0.166		
23	TYR		0.286		
39	GLY	-0.484	0.340	-0.482	0.446
41	TYR	-0.290	0.209	-0.269	0.260
47	HIS	-0.319	0.245	-0.265	0.225
51	HIS		-0.145		
52	VAL		0.174		
55	GLY	-0.257	0.195		
62	GLY	-0.492	0.347	-0.700	0.584
65	ILE	-0.574		-0.714	
66	GLU				0.318
74	LYS	0.109	-0.081		
76	LEU	0.034	-0.042		
77	ILE	-0.247		0.113	-0.079
79	TYR	-0.317	0.218	-0.262	0.221
82	GLY	-0.097	0.092	-0.079	0.061
98	LEU	0.028	-0.032	0.135	-0.092
108	ALA	0.098	-0.041	0.089	-0.066
110	GLN	0.114	-0.073	0.137	-0.112
112	LYS	0.100	-0.073	0.144	-0.121
114	GLY	0.117	-0.076	0.182	-0.157
115	LEU	0.100	-0.072		
116	PHE	0.120	-0.075	0.193	-0.173
117	LYS	0.114	-0.081		
121	GLY	0.071	-0.049	0.130	-0.121
122	THR	0.065	-0.046	0.121	-0.111
123	ILE	0.089	-0.064	0.177	-0.151
127	SER	0.202	-0.108	0.264	-0.205
128	LEU	0.284	-0.178	0.386	-0.316
129	ASP	0.377	-0.222	0.435	-0.355
139	ILE	0.065			
140	VAL	0.032	-0.025	0.119	-0.088
142	LYS	0.032	-0.041	0.071	-0.049
148	GLY	-0.001	-0.005	0.128	-0.088
164	ALA	0.259	-0.175	0.527	-0.425
165	ILE	0.131		0.305	
166	ALA	0.136	-0.070		

<sup>a</sup> See footnote a of Table S1.

**Table S3.** PCSs in ppm of backbone amide protons of  $^{15}\text{N}$ -labeled DENpro Ser68Cys (mutant C) tagged with C1 or C2 loaded with  $\text{Tb}^{3+}$  or  $\text{Tm}^{3+}$  <sup>a</sup>

Residue	C1		C2	
	$\text{Tb}^{3+}$	$\text{Tm}^{3+}$	$\text{Tb}^{3+}$	$\text{Tm}^{3+}$
55* ARG	0.048	-0.039	-0.764	0.431
56* ALA	0.036	-0.007		0.328
57* ALA	0.043	-0.014	-0.436	0.268
60* ARG	0.022	-0.017	-0.243	0.117
62* GLU	0.008	-0.005	-0.084	0.059
63* GLU	0.012			
64* GLN	-0.004	-0.021		
65* ALA			-0.060	0.039
70* SER	-0.023	0.022		
71* SER	-0.012	0.013	0.012	
75* SER	-0.008	0.013	0.076	-0.062
78* ILE	-0.020	0.040		
79* SER	-0.083	0.059	0.355	-0.209
85* SER			0.226	-0.102
21 GLY	0.195			0.378
24 ARG	0.022			
26 LYS	-0.177	0.172		0.541
28 LYS	-0.201	0.146	-0.510	0.285
34 SER	-0.134	0.110		
39 GLY	-0.148	0.138		
50 TRP				-0.209
51 HIS		0.437	0.491	-0.275
52 VAL	-0.493	0.415	0.051	-0.023
53 THR	-0.616	0.504	-0.238	0.145
62 GLY	-0.065	0.054		
85 LEU				0.042
87 GLY	-0.190	0.183		
89 TRP		-0.017		
96 GLN	-0.012	0.002		
98 LEU	-0.039	0.035	-0.143	0.093
100 LEU	-0.075	0.075	-0.271	0.147
103 GLY			-0.237	0.143
104 LYS	-0.049	0.041	-0.203	0.116
108 ALA	-0.008	0.013		
110 GLN	-0.009	0.016	-0.053	0.030
111 THR	-0.016	0.009		
114 GLY	-0.021	0.019	0.040	-0.029
115 LEU	-0.007	0.015		

116	PHE	-0.017	0.019	0.091	-0.069
117	LYS	-0.005	0.008	0.109	-0.070
121	GLY	0.043	-0.033	0.153	-0.108
122	THR	0.042	-0.029	0.112	-0.095
123	ILE	0.000	0.007	0.113	-0.084
127	SER	-0.031	0.024	0.004	-0.009
128	LEU	-0.051	0.049		
131	SER	-0.069	0.071	-0.097	0.048
133	GLY	-0.118	0.107	-0.120	0.070
140	VAL	-0.013	0.021	-0.070	0.056
148	GLY	-0.046	0.058	-0.042	0.031
162	VAL	-0.065	0.062	0.086	-0.041
163	SER	-0.062	0.073		
164	ALA	-0.099	0.090	0.131	-0.076
166	ALA	-0.134	0.120	0.059	-0.048

<sup>a</sup> See footnote a of Table S1.

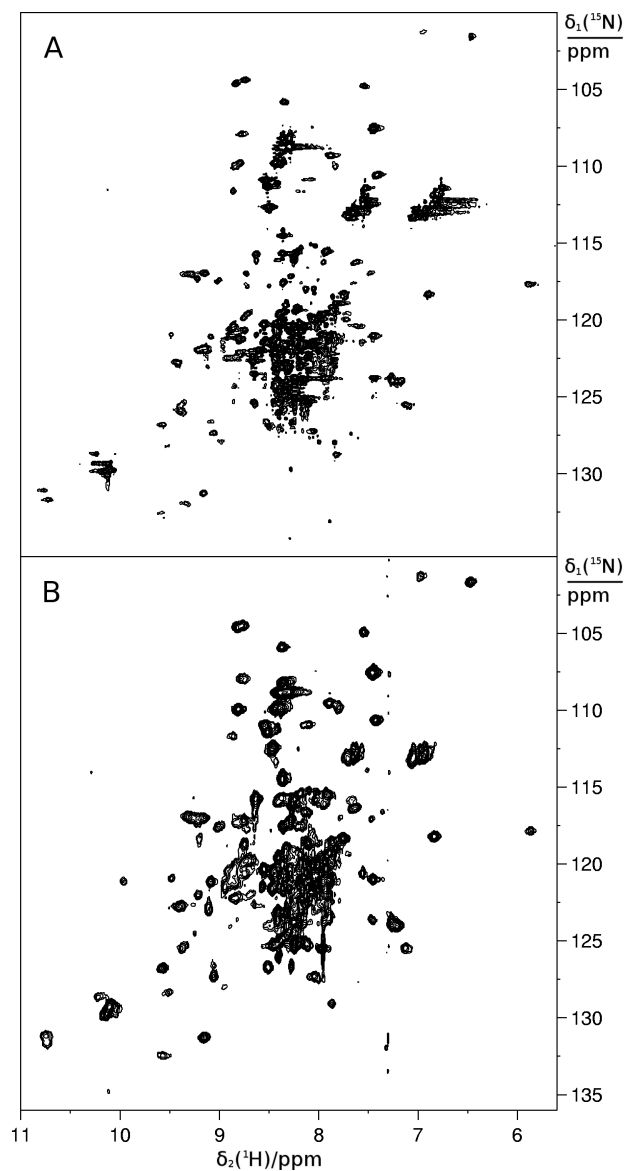


**Figure S5.** Inhibitor **1** does not bind to the Ser135Ala mutant of DENpro. The figure shows <sup>15</sup>N-HSQC spectra of uniformly <sup>15</sup>N-labeled samples of (A) the wild-type protein in the absence of an inhibitor and (B) the DENpro mutant Ser135Ala in the presence of a five-fold excess of **1**. The similarity between the two spectra and, particularly, the absence of cross-peaks appearing in wild-type protein in the presence of inhibitors (compare Figure 3B) indicates that **1** does not bind to the Ser135Ala mutant.

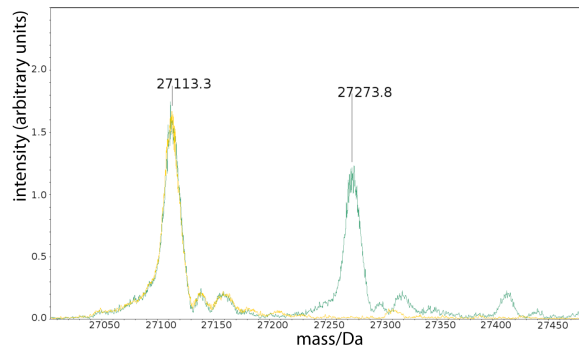


**Figure S6.** The p-guanidino-benzoyl moiety of inhibitor **1** binds covalently to DENpro. The figure shows a superimposition of mass spectra of DENpro recorded on a Bruker FT-ICR spectrometer. The samples were prepared with (green) and without (yellow) inhibitor **1**. The mass difference between the two peaks is 160.5 Da (expected for  $C_8ON_3H_7$ : 161).

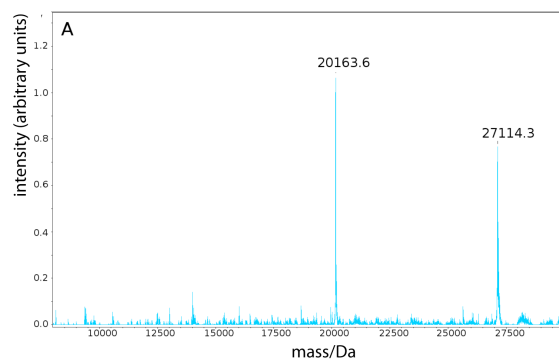


**Figure S7.** DENpro is prone to self-cleavage following Trp5 in NS3. Mass spectrum of DENpro (mutant Lys15Ala). The mass of 20163.6 corresponds to the C-terminal fragment of the NS2B-NS3pro construct following cleavage after Trp5.

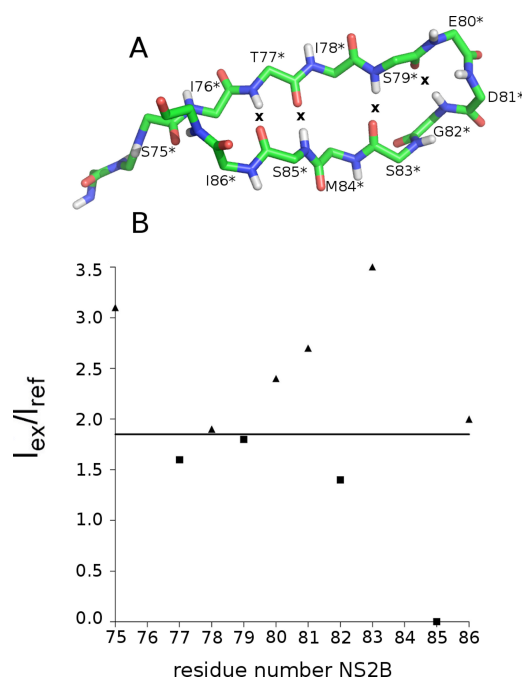


**Figure S8.** Assessing the structural conservation of the  $\beta$ -hairpin of NS2B-C by amide proton exchange. (A) Structure of the  $\beta$ -hairpin of NS2B-C of DENpro modelled on the NS2B-C structure observed in the closed conformations of WNVpro. Nitrogen atoms are in blue, oxygen atoms in red and hydrogen bonds are indicated by crosses. Only the backbone  $C^\alpha$  atoms and amides are shown. (B) Intensities of 3D NOESY- $^{15}\text{N}$ -HSQC cross-peaks observed at the water chemical shift in the presence of a five-fold excess of **1**. The spectrum was recorded at 25 °C in a 20 mM MES buffer at pH 6.5 containing 30 mM NaCl. The cross-peak intensities were normalized by their intensities in a reference  $^{15}\text{N}$ -HSQC spectrum. Cross-peak intensities of hydrogen bonded and non-hydrogen bonded amides are indicated by boxes and triangles, respectively. The horizontal line indicates that H-bonded amide protons exchange more slowly. More intense cross-peaks would have been expected for the solvent exposed amide protons of Ile78\* and Ile86\*. It is well known, however, that the branched side chains of isoleucine residues reduce the amide proton exchange rates of the backbone amides more than any other amino acid side chain.<sup>24</sup>

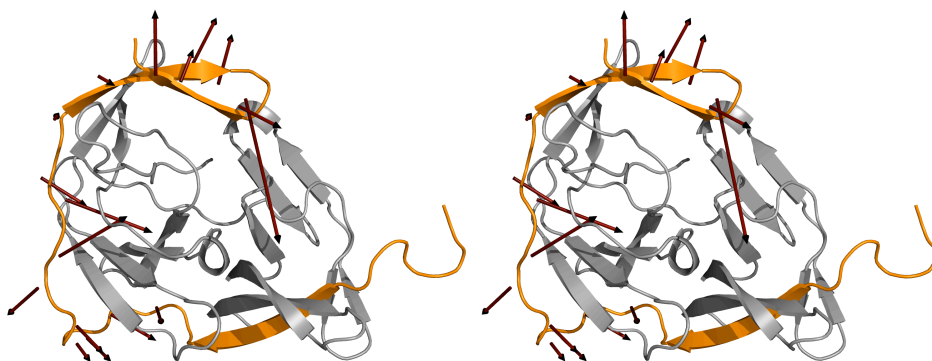


**Figure S9.** Direction of structural changes of NS2B that could lead to an improved fit of experimental and back-calculated PCSs. The stereo figure displays the directions of the gradients of steepest descent of PCS quality factors for individual amide protons in NS2B. The local PCS quality factor is defined as

$$Q_{local} = \sqrt{M^{-1} \sum (PCS_{calc} - PCS_{exp})^2} / \sqrt{N^{-1} \sum PCS_{exp}^2},$$

where  $M$  is the number of all  $PCS_{exp}$  values that could be measured for the individual spin in the twelve paramagnetic samples and  $N$  is the total number of  $PCS_{exp}$  values measured in NS2B.  $PCS_{calc}$  values were back-calculated from the  $\Delta\chi$  tensors that had been established by the PCSs of NS3pro (Table 1) using the model of the closed state (Figure 1B). The length of each arrow is proportional to the steepness of the local gradient, with an arrow length of 1 Å corresponding to 0.01/Å. The figure shows that adjusting the conformation of NS2B by following the gradients of the local PCS quality factors would in several instances lead to steric clashes with NS3pro. This suggests that further structure refinement is limited by inaccuracies in the  $\Delta\chi$  tensor determinations.

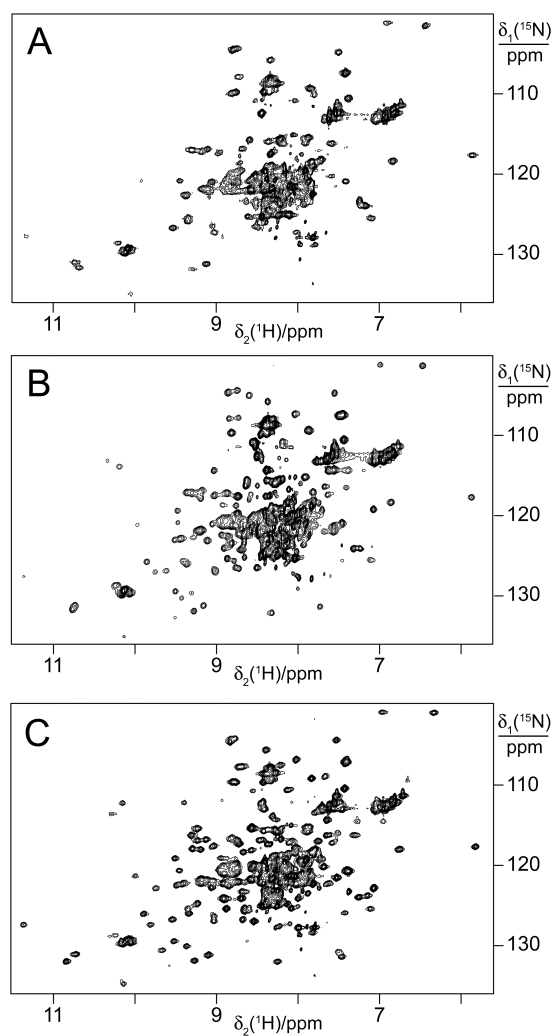


**Figure S10.** A similar appearance of the  $^{15}\text{N}$ -HSQC spectra suggests that inhibitors **1** and **2** similarly induce the closed state in DENpro. The figure shows  $^{15}\text{N}$ -HSQC spectra of 1 mM solutions of uniformly  $^{15}\text{N}$ -labeled DENpro with and without inhibitors at pH 6.9 and 25 °C. The spectra were recorded on a Bruker 800 MHz NMR spectrometer. (A) DENpro without inhibitor. The spectrum is identical to that shown in Figure 3A of the main text. (B) DENpro with a 5-fold excess of inhibitor **1**. The spectrum is identical to that shown in Figure 3B. (C) DENpro with a 20% excess of inhibitor **2**, added from a 100 mM stock solution in DMSO.

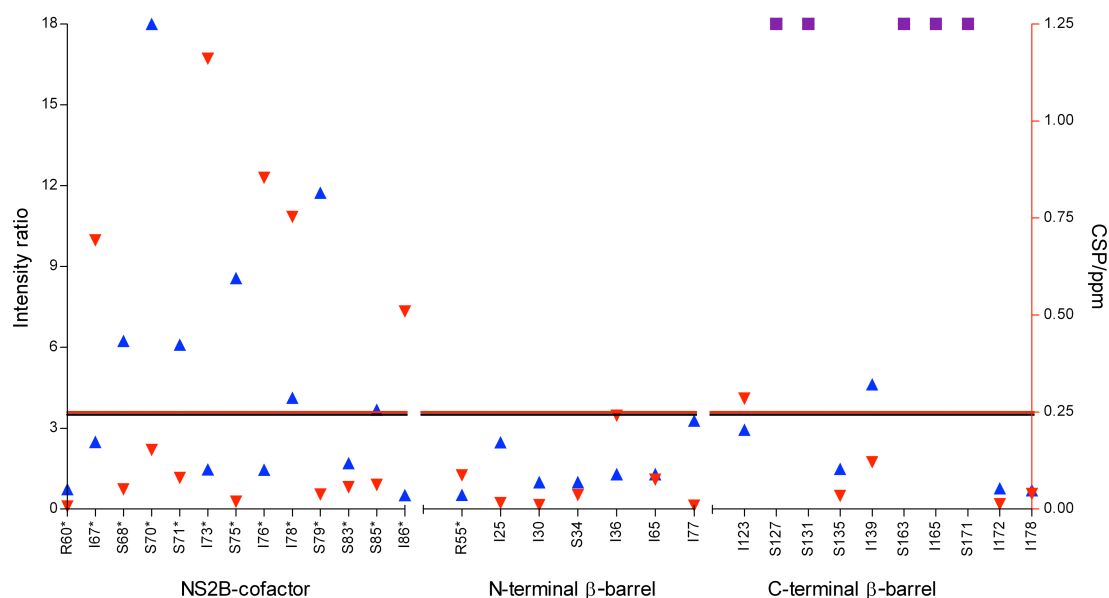


**Figure S11.** Changes in  $^{15}\text{N}$ -HSQC cross-peak heights and chemical shifts upon addition of inhibitor **1**. Blue triangles indicate the ratio of peak heights observed with and without inhibitor. Red triangles display the chemical shift perturbation (CSP) upon addition of inhibitor. The CSP was calculated as  $[(\Delta\delta_{\text{H}})^2 + (\Delta\delta_{\text{N}})^2/5]^{0.5}$ , where  $\Delta\delta_{\text{H}}$  and  $\Delta\delta_{\text{N}}$  are the change in chemical shift in the  $^1\text{H}$  and  $^{15}\text{N}$  dimension of the  $^{15}\text{N}$ -HSQC spectrum. Purple squares mark residues for which cross-peaks could only be identified in the presence of inhibitor (they are probably broadened beyond detection in the absence of **1**). Horizontal lines mark the cut-off values (at an intensity ratio of 1.5 and a CSP of 0.25 ppm) used to color code Figure 4.

**Table S4.** Backbone amide  $^1\text{H}$  and  $^{15}\text{N}$  chemical shifts of DENpro with 5-fold excess of inhibitor **1** at pH 6.5 and 25 °C

E54*	8.61	120.3	S34	8.53	114.7
R55*	9.41	131.7	Q35	8.59	121.8
A56*	8.92	126.0	I36	8.31	119.1
A57*	7.57	115.4	A38	8.71	122.6
D58*	8.49	119.4	G39	8.75	103.8
V59*	8.85	120.8	V40	8.40	115.4
R60*	7.11	123.0	Y41	10.05	134.2
W61*	8.65	121.3	H47	8.00	126.4
E62*	9.18	131.0	T48	8.93	116.6
E63*	8.78	124.4	W50	7.35	124.8
Q64*	8.65	116.7	H51	10.11	113.1
A65*	7.36	122.7	V52	6.76	117.5
S68*	8.84	119.5	T53	6.37	100.5
S70*	7.47	113.5	R54	8.96	120.3
S71*	8.33	112.1	G55	6.90	100.5
I73*	8.05	117.1	A56	7.35	120.1
S75*	8.84	117.8	G62	8.67	103.6
I76*	8.25	118.8	R64	8.33	122.8
T77*	8.78	116.3	I65	9.26	124.7
I78*	8.68	125.6	E66	8.57	124.2
S79*	8.81	123.2	68E	8.55	121.1
E80*	8.71	120.2	W69	7.84	122.9
D81*	7.52	113.4	A70	7.03	124.7
G82*	7.94	106.5	D71	7.55	116.7
S83*	8.14	115.0	K73	7.60	118.4
M84*	8.66	120.6	K74	7.32	115.6
S85*	8.28	113.1	D75	7.92	116.6
I86*	8.74	122.5	L76	7.71	116.2
G21	8.75	107.0	I77	8.65	117.8
A22	9.35	121.9	Y79	9.39	120.0
Y23	9.42	122.2	G82	8.28	105.0
R24	9.13	116.4	L85	5.77	116.8
I25	8.63	120.2	E86	9.10	121.0
K26	9.53	125.9	G87	7.75	108.4
K28	9.07	130.4	E88	8.88	122.0
G29	7.82	114.4	W89	9.42	128.7
I30	8.36	120.1	94G	8.22	108.3
L31	8.24	118.1	V95	8.72	108.9
G32	7.35	106.6	Q96	9.07	115.8
Y33	7.80	-	V97	8.82	120.3

L98	8.23	131.2	S131	8.93	113.4
A99	7.91	123.4	G133	8.20	107.3
L100	7.90	128.0	V140	9.76	124.7
G103	8.79	111.2	D141	8.75	121.4
K104	7.73	117.6	K142	7.86	115.3
R107	7.96	121.4	G144	8.70	108.9
A108	8.41	125.6	K145	8.45	119.1
Q110	9.32	129.3	V146	8.93	121.9
T111	9.09	117.0	V147	8.15	119.6
K112	7.91	126.8	G148	7.45	103.9
G114	8.63	106.9	L149	9.29	116.3
L115	8.50	117.1	G159	10.2	112.2
F116	9.38	118.4	A160	7.22	123.3
K117	9.19	121.7	V162	8.06	125.2
T118	8.15	114.9	S163	8.48	116.4
T120	8.09	107.3	A164	9.21	128.8
G121	7.40	109.4	I165	7.58	121.2
T122	8.55	115.4	A166	7.59	130.4
I123	9.02	122.3	K170	8.33	122.2
G124	8.08	109.8	S171	8.63	119.1
A125	8.27	122.0	I172	8.25	122.4
V126	9.20	116.4	I182	7.94	119.1
S127	9.67	126.2	F183	8.08	119.7
L128	6.98	118.3	R184	7.93	118.8
D129	8.70	124.7	K185	8.03	118.9
F130	7.47	121.1			

## References

- (1) Erbel, P.; Schiering, N.; D'Arcy, A.; Renatus, M.; Kroemer, M.; Lim, S. P.; Yin, Z.; Keller, T. H.; Vasudevan, S.G.; Hommel, U. *Nat. Struct. Mol. Biol.* **2006**, *13*, 372-373.
- (2) Wu, P. S. C.; Ozawa, K.; Lim, S. P.; Vasudevan, S.; Dixon, N. E.; Otting, G. *Angew. Chemie Int. Ed.* **2007**, *46*, 3356-3358.
- (3) Sivashanmugam, A.; Murray, V.; Cui, C.; Zhang, Y.; Wang, J.; Li, Q. *Protein Sci.* **2009**, *18*, 936-948.
- (4) Schoepfer, R. *Gene* **1993**, *124*, 83-85.
- (5) Apponyi, M.; Ozawa, K.; Dixon, N. E.; Otting, G. *Methods Mol. Biol.* **2008**, *426*, 257-268.
- (6) Klammt, C.; Löhr, F.; Schäfer, B.; Haase, W.; Dötsch, V.; Rüterjans, H.; Glaubitz, C.; Bernhard, F. *Eur. J. Biochem.* **2004**, *271*, 568-580.
- (7) Neylon, C.; Brown, S. E.; Kralicek, A. V.; Miles, C. S.; Love, C. A.; Dixon, N. E. *Biochemistry* **2000**, *39*, 11989-11999.
- (8) Graham, B.; Loh, C. T.; Swarbrick, J. D.; Ung, P.; Shin, J.; Yagi, H.; Jia, X.; Chhabra, S.; Pintacuda, G.; Huber, T.; Otting, G. *Bioconj. Chem.* **2011**, DOI: 10.1021/bc200353c
- (9) Ozawa, K.; Headlam, M. J.; Schaeffer, P. M.; Henderson, B. R.; Dixon, N. E.; Otting, G. *Eur. J. Biochem.* **2004**, *271*, 4084-4093.
- (10) Su, X. C.; Loh, C. T.; Qi, R.; Otting, G. *J. Biomol. NMR* **2011**, *50*, 35-42.
- (11) Ekonomiuk, D.; Su, X. C.; Ozawa, K.; Bodenreider, C.; Lim, S. P.; Otting, G.; Huang, D.; Caflisch, A. *J. Med. Chem.* **2009**, *52*, 4860-4868.
- (12) Wu, P. S. C.; Ozawa, K.; Jergic, S.; Su, X. C.; Dixon, N. E.; Otting, G. *J. Biomol. NMR* **2006**, *34*, 13-21.
- (13) Jia, X.; Ozawa, K.; Loscha, K.; Otting, G. *J. Biomol. NMR* **2009**, *44*, 59-67.
- (14) Aleshin, A. E.; Shiryaev, S. A.; Strongin, A. Y.; Liddington, R. C. *Protein Sci.* **2007**, *16*, 795-806.
- (15) Sali, A.; Blundell, T. L. *J. Mol. Biol.* **1993**, *234*, 779-815.
- (16) Eswar, N.; Marti-Renom, M. A.; Webb, B.; Madhusudhan, M. S.; Eramian, D.; Shen, M.; Pieper, U.; Sali, A. *Current Protocols in Bioinformatics* **2006**, Wiley, Supplement 15, 5.6.1-5.6.30.
- (17) Robin, G.; Chappell, K.; Stoermer, M. J.; Hu, S.; Young, P. R.; Fairlie, D. P.; Martin, J. L. *J. Mol. Biol.* **2009**, *385*, 1568-1577.
- (18) Thompson, J. D.; Gibson, T. J.; Plewniak, F.; Jeanmougin, F.; Higgins, D. G. *Nucl. Acids Res.* **1997**, *25*, 4876-4882.
- (19) Shen, M. Y.; Sali, A. *Protein Sci.* **2006**, *15*, 2507-2524.
- (20) Wichapong, K.; Pianwanit, S.; Sippl, W.; Kokpl, S. *J. Mol. Recognit.* **2009**, *23*, 283-300.
- (21) Bertini, I.; Luchinat, C.; Parigi, G. *Prog. Nucl. Magn. Reson. Spectrosc.* **2002**, *40*, 249-273.
- (22) Nguyen, T. H. D.; Ozawa, K.; Stanton-Cook, M.; Barrow, R.; Huber, T.; Otting, G. *Angew. Chemie Int. Ed.* **2011**, *50*, 692-694.

- (23) Schmitz, C.; Stanton-Cook, M. J.; Su, X. C.; Otting, G.; Huber, T. *J. Biomol. NMR* **2008**, *41*, 179-189.
- (24) Bai, Y.; Milne, J. S.; Mayne, L.; Englander, S. W. *Proteins* **1993**, *17*, 75-86.